0026-895X/95/020268-12$3.00/0

MOLECULAR PHARMACOLOGY, 48:268–279 (1995).

The Low Efficacy γ-Aminobutyric Acid Type A Agonist 5-(4-Piperidyl)isoxazol-3-ol Opens Brief Cl^- Channels in Embryonic Rat Olfactory Bulb Neurons

UFFE KRISTIANSEN, JEFFERY L. BARKER, and RUGGERO SERAFINI

Department of Biological Sciences, Royal Danish School of Pharmacy, Copenhagen, Denmark 2100 (U.K.), and Laboratory of Neurophysiology, National Institute of Neurological Disorders and Stroke, National Institutes of Health, Bethesda, Maryland 20892 (J.L.B., R.S.)

Received February 1, 1995; Accepted May 26, 1995

SUMMARY

4-PIOL is a structural analog of GABA that has low efficacy at $GABA_A$ receptor Cl^- channels and activates a nondesensitizing Cl^- conductance in central neurons. We investigated the biophysical mechanisms of its low efficacy in embryonic olfactory bulb neurons, which express a limited number of $GABA_A$ receptor subunit transcripts. Spectral analysis of GABA- and 4-PIOL-induced current fluctuations evoked in whole-cell recordings showed that three components with mean durations of ~0.7, 5, and 50 msec adequately describe the kinetics of the responses induced by both ligands. The contribution of the longest-lasting component was ~60% in the spectra of GABA-evoked responses but <3% in the spectra of 4-PIOL-evoked responses. This is interpreted as a low incidence of long-lasting bursts in 4-PIOL-evoked responses. No difference was evident between the average inferred unitary conductances for 4-PIOL- and GABA-induced channels. These results at the level of the whole cell were confirmed and extended in outside-out single channel recordings. Taken together, the results indicate that the mechanism responsible for the low efficacy of 4-PIOL is the inability to produce frequent bursts of long duration.

4-PIOL, a structural analog of GABA (Fig. 1), is a relatively weak $GABA_A$ agonist on cat spinal neurons, antagonizes muscimol-stimulated benzodiazepine binding to rat cortical membranes, and is a low efficacy, nondesensitizing partial agonist at $GABA_A$ receptors on cultured rat hippocampal neurons (reviewed in Ref. 1). A comparison of the biophysical properties of the Cl^- channels gated by 4-PIOL and GABA may reveal the molecular correlates of the mixed agonist-antagonist profile of 4-PIOL and offer clues to the synthesis of clinically valuable structural analogs with similar nondesensitizing effects (1). We used whole cell and excised outside-out patch-clamp recordings of acutely dissociated embryonic rat OB cells to investigate the biophysical properties of the $GABA_A$ receptor channels activated by GABA and 4-PIOL. We used embryonic day 15 OB cells because the $GABA_A$ receptors are derived from mRNAs encoding a limited number of $GABA_A$ receptor subunits ($\alpha 2$, $\beta 2$, and $\beta 3$) as detected by *in situ* hybridization (2, 3). The limited subunit expression would be expected to result in relatively reduced variability of Cl^- channel properties coupled to $GABA_A$ receptors. The small size of these cells is also a useful feature in noise analysis to achieve a more accurate resolution of high frequency events.

In the present study, we a) studied the pharmacology of GABA- and 4-PIOL-activated Cl^- currents, b) used fluctuation analysis to calculate spectra of 4-PIOL- and GABA-evoked Cl^- current noise, c) measured directly the elementary properties of agonist-activated Cl^- channels in excised outside-out patches, and d) compared the biophysical parameters of channels measured in patches with those inferred by fluctuation analysis. We show that the very low efficacy of 4-PIOL correlates with its inability to trigger long-lasting bursts.

Materials and Methods

Cell dissociation. Pregnant Sprague-Dawley rats (Taconic Farms, Germantown, NY) were killed through CO_2-induced anoxia in a box containing dry ice (frozen CO_2). Embryos were rapidly removed and placed in phosphate buffered saline. A standard atlas (4) was used as a reference to determine embryonic age according to crown–rump-length measurement and to identify the OBs. Embryonic day 15 embryos typically exhibited crown–rump-length of 11–13 mm. After dissection at room temperature, we incubated the OBs for 30–40 min at 37° in EBSS containing 20 U/ml papain (Boehringer Mannheim, Indianapolis, IN) and 0.5 mM EDTA tetrasodium. Tissue

This work was supported by travel grants from the Carlsberg Foundation, Copenhagen, Denmark, and the Danish Medical Research Council (U.K.).

ABBREVIATIONS: GABA, γ-aminobutyric acid; 4-PIOL, 5-(4-piperidyl)isoxazol-3-ol; THIP, 4,5,6,7-tetrahydroisoxazolo[5,4-c]pyridin-3-ol; HEPES, 4-(2-hydroxyethyl)-1-piperazine ethanesulfonic acid; EBSS, Earle's balanced salt solution, EGTA, ethylene glycol bis(β-aminoethyl ether)-*N,N,N′,N′*-tetraacetic acid; OB, olfactory bulb; BSA, bovine serum albumin.

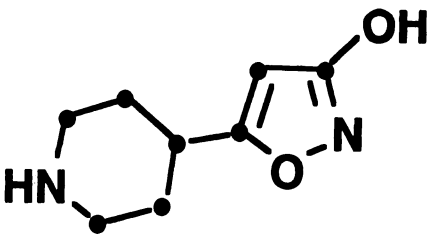

4-PIOL

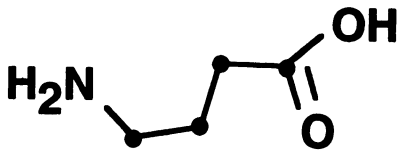

GABA

Fig. 1. Structures of GABA and 4-PIOL.

was then centrifuged at low speed and resuspended in 3 ml EBSS containing 1 mg/ml fatty acid-free BSA (Sigma Chemical Co., St Louis, MO) and 1 mg/ml trypsin inhibitor (Sigma Chemical Co.). After gentle trituration with a plastic pipette, we allowed macroscopic fragments of undissociated tissue to settle by gravity to the bottom of a centrifuge tube, and the supernatant, enriched in dissociated embryonic cells, was carefully layered on a solution of EBSS containing 10 mg/ml BSA and 10 mg/ml trypsin inhibitor and then centrifuged at 800 × *g* for 10 min to separate cells from debris. The resulting pellet of cells was resuspended again in EBSS and eventually plated at 37° on the uncoated or polylysine-coated surface of 35-mm-diameter plastic Petri dishes. Electrophysiological recordings were always begun at least 1 hr after plating, when cells had become adherent to the dish, and continued over a period of 6–9 hr.

Solutions. The extracellular solution used in the present study contained 140 mM NaCl, 5 mM KCl, 2 mM $CaCl_2$, 1 mM $MgCl_2$, 10 mM glucose, and 10 mM HEPES-NaOH. The intracellular pipette solution contained 145 mM CsCl, 2 mM $MgCl_2$, 1.1 mM EGTA, 0.1 mM $CaCl_2$, 10 mM HEPES-CsOH, and 5 mM Mg-ATP. Osmolarity and pH were adjusted in all solutions, if necessary, to 300–320 mOsmol/kg and 7.2–7.3, respectively. GABA and bicuculline methobromide were obtained from Sigma Chemical Co. 4-PIOL hydrobromide was provided by Prof. P. Krogsgaard-Larsen (Dept. of Organic Chemistry, Royal School of Pharmacy, Copenhagen, Denmark) Stock solutions were made of 100 mM GABA, 10 mM bicuculline methobromide, and 100 mM 4-PIOL hydrobromide in distilled water and refrigerated at 20° for as long as 2 weeks.

Drug application. Stock solutions were diluted with extracellular solution and applied to the cell via low pressure from closely positioned micropipettes. In experiments involving fluctuation analysis or single-channel recording, GABA and 4-PIOL were applied for at least 1 min, whereas in experiments involving only concentration-response studies, applications of 4-PIOL were continued for at least 30 sec. Because 4-PIOL-evoked currents consistently had low amplitude (≤10 pA), to obtain a better resolution of current fluctuations, we used asymptotic concentrations of 4-PIOL. Low concentrations of GABA in fluctuation analysis experiments were chosen that corresponded to <1% of the maximal response to stimulate responses that were comparable in amplitude to those of 4-PIOL and that were either nondesensitizing or slowly desensitizing.

Whole-cell recording. EBSS was replaced with the extracellular medium. Pipettes made of thin glass with filament (1.5 mm o.d.; WPI, Sarasota, FL) were pulled with a computerized BB-CH-PC puller (Mecanex, Geneva, Switzerland). In extracellular medium, the range of tip resistances was 2–5 MΩ. Intracellular recordings were performed with the use of whole-cell patch-clamp techniques at room temperature (21–22°). Pipette currents were monitored with the use of an Ag-AgCl wire and amplified through an Axopatch 200 amplifier (Axon Instruments, Foster City, CA) in the resistive headstage mode. Series resistance was <10 MΩ and was 50–80% compensated. The voltage error was <5 mV. At the highest concentrations of the GABA concentration-response experiments, series resistance compensations of ≤95% were obtained by adjusting the lag control of the low-pass filter in the current feedback loop to 80 μsec. Recordings with ≤8–9-mV voltage error were included in the data. Signals were low-pass filtered at 3 kHz with an eight-pole Bessel filter (902 Frequency Devices, Haverhill, MA), digitized at 18 kHz through a CRC VR-100A Digital Recorder (Instrutech Corp., Mineola, NY), and stored on video tape.

Analysis of concentration-response experiments. Current responses to several short applications of different GABA and 4-PIOL concentrations were measured and expressed relative to the response to 2 μM GABA and 100 μM 4-PIOL GABA on the same cell. Mean currents were calculated using Strathclyde Electrophysiological Software (University of Strathclyde, Glasgow, UK). A logistical function was fitted to the experimental data using the software Kaleidagraph on a Macintosh computer. It had the form $R = (R_{max}\text{-}C^n)/(EC_{50}{}^n + C^n)$, where R is the relative current response, C is the concentration of 4-PIOL, EC_{50} is the concentration inducing a half-maximal response, and n is the Hill coefficient.

Fluctuation analysis of agonist-activated whole cell currents. Data were played back, low-pass filtered at 1 kHz through the eight-pole Butterworth filter, high-pass filtered at 0.1 Hz through a homemade filter, and digitized at 2 kHz through a National Instruments LAB PC (National Instruments Corp., Austin, TX) acquisition board. Data were analyzed with Strathclyde Electrophysiological Software. The power density spectrum of current variance in the baseline periods was calculated and then subtracted from those calculated during agonist-induced currents. The resulting "difference spectra" were fitted with one or more Lorentzian functions of the form $S(f) = S(0)/[1 + (f/f_c)^2]$, where f is the frequency, $S(f)$ is the spectral density, $S(0)$ is the value of S at zero frequency, and f_c is the corner frequency. Spectral density plots were fitted using the software Kaleidagraph (Synergy Software, Reading, PA) on a Macintosh computer. The number of components was increased until the fit was not significantly improved by additional components, as determined with an F test. The variance, σ^2, of the agonist-induced current fluctuations was $\sigma^2 = \int S(f)df$. In each nth component, the variance $\sigma_n{}^2$ was $\sigma_n{}^2 = (\pi S(0)f_c)/2$ and the relative contribution C_n to the total variance in the fluctuations was $C_n = S(0)_{(n)}f_{c(n)}/\Sigma(S(0)f_c)$, where $S(0)_{(n)}$ and $f_{c(n)}$ are the asymptote in power and the corner frequency of the n^{th} Lorentzian function, respectively, and $\Sigma\,(S(0)f_c)$ is the sum of the products (asymptote) (corner frequency) of each Lorentzian component. The mean duration, τ, of each exponential component of the channel kinetics is expressed as $\tau = (2\pi f_c)^{-1}$. The conductance, γ, can be estimated (5) from the relationship $\gamma = \sigma^2/m_I(V-V_{eq})$, where σ^2 is the agonist-induced variance, m_I is the agonist-induced mean membrane current change, and $V-V_{eq}$ is the difference between the holding potential and the equilibrium potential for the ionic conductance associated with the response. The electrode series resistance R and the whole-cell capacitance C have the effect of a filter with a −3-dB effect at the frequency $f = 1/2\pi RC$. Because the range of cell capacitance values is small (1.5–10 pF), f is always higher than the effective bandwidth of our recordings.

Outside-out single channel recordings. EBSS was replaced with the extracellular medium. Pipette tips were routinely coated with Sylgard 184 (Dow Corning, Midland, MI) and polished with a Narishige MF-9 (Narishige, Tokyo, Japan) microforge. In extracellular medium, the range of tip resistances was 8–12 MΩ. After establishment of the outside-out configuration, the recording pipette was placed just under the surface of the recording medium to decrease noise. Holding potentials of −60 or −80 mV were used for single channel recording. Patch currents were amplified with an Axopatch 200 (Axon Instruments, Foster City, CA) in the capacitative headstage mode, low-pass filtered at 3 kHz through an eight-pole Bessel filter, digitized at 18 kHz, and stored on video tape. For analysis, recordings were replayed, low-pass filtered at 1 kHz through an eight-pole Bessel filter, and digitized through a Labmaster board (Axon Instruments) at a sampling rate of 200 μsec per point. The effective bandwidth of the recording system was calculated as follows: $1/(f_c)^2 = [1/(f_1)^2] + [(1/(f_2)^2]$, where f_1 and f_2 are the cutoff frequencies of two filters in series; f_c was 970 Hz. The corresponding rise time was ~340 μsec. It was calculated as follows (6): T_d (dead time) = $0.179/f_c$, T_r (rise time) = $T_d/0.538$, where f_c is the bandwidth. Data were analyzed with pCLAMP software version 5.5 (FETCHAN and pSTAT; Axon Instruments). A detection threshold of 50% of the preferred amplitude level was used as an event-finder scheme. The analysis was carried out by the operator directly examining each opening and, in case of drift or artifacts, correcting baseline level and the opening channel step amplitude before storing the data.

Patches were used only if at the effective bandwith of 970 Hz, the 50% threshold for the 19-pS subconductance level was at least 3.5 times the root mean square of the baseline noise; the rate of false events was maintained at 1–2 orders of magnitude lower than the rate of channel events (6). For amplitude analysis, events shorter than twice the rise time of the system were disregarded.

Dwell-time analysis was restricted to runs of single-channel current where detectable openings to conductance states other than the main conductance state were rare. Openings to other than the main conductance level were excluded together with adjacent closed intervals. Events shorter than the rise time were excluded (6).

Some patches exhibited spontaneous channel openings of short duration to the same conductance state as GABA-gated channels. These spontaneous currents disappeared at 0 mV. Sometimes these openings disappeared within 1 min; otherwise, the patch was not used. Other patches exhibited no channel activity when GABA was applied.

Bursts were defined as sets of one or more openings separated by closures shorter than a critical time t_c. t_c was determined according to Colquhoun and Sakmann (7). For GABA, the two shortest closed times were defined as intraburst closed times, whereas for 4-PIOL, the shortest of the three closed-time components was considered intraburst closed time. The sufficient numbers of components fitting open-time, closed-time, and burst-length distributions were defined by an F test.

Statistical analysis. Values are given as mean ± standard error.

Results

4-PIOL Is a Low Efficacy, Nondesensitizing Agonist at the $GABA_A$ Receptor Cl^- Channel that Blocks Activation by GABA of the Receptor-Channel Complex

Changing the holding potential showed that the macroscopic current response and associated fluctuations induced by 4-PIOL disappeared at 0 mV and reappeared at positive potentials (Fig. 2). Because the theoretical equilibrium potential for Cl^- ions was at or near 0 mV, we conclude that the current was due to movement of Cl^- ions. The current response induced by 0.3 (n = 4) and 1 (n = 3) mM 4-PIOL was abolished by 100 μM bicuculline (Fig. 2). Taken together, the results indicate that 4-PIOL is an agonist at the $GABA_A$ receptor-Cl^- channels expressed by embryonic OB neurons. The concentrations of 4-PIOL necessary to activate the $GABA_A$ receptor were relatively high: 10 μM 4-PIOL elicited just-detectable changes in membrane current; even 1 mM 4-PIOL evoked currents that were modest in amplitude, 7.1 ± 0.7 pA (n = 4). The EC_{50} was 31 ± 8 μM, which is significantly lower than that in cultured hippocampal neurons (3). The Hill coefficient was 1.05 ± 0.27. In contrast, GABA was consistently effective at concentrations as low as 0.5 μM. The maximal effect occurred at 1 mM GABA (Fig. 3B), which evoked currents of 9.2 ± 4.1 nA (n = 6). The concentration-response curve of the GABA-evoked current responses could be fitted with a logistic equation with an EC_{50} of 150 ± 30 μM and a Hill cofficient of 1.4 ± 0.4.

Although 4-PIOL was an agonist at the $GABA_A$ receptor-Cl^- channels, it also antagonized GABA-induced current re-

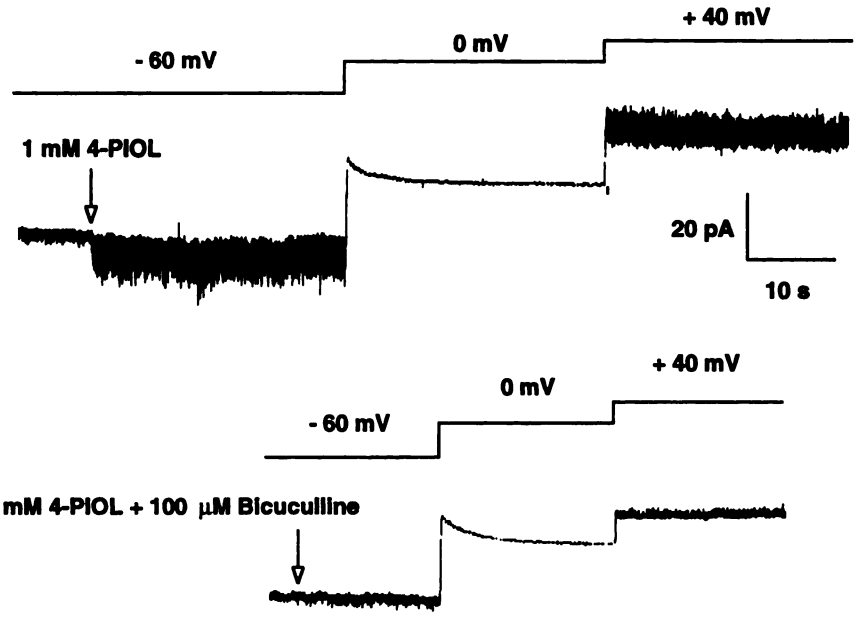

Fig. 2. 4-PIOL induces a microscopic current response that is blocked by bicuculline. *Top*, 1 mM 4-PIOL induces a highly fluctuating current recorded whole cell at a holding potential of −60 mV. Current fluctuations disappear entirely at 0 mV and reappear at +40 mV. *Bottom*, in the presence of 100 μM bicuculline methobromide, 4-PIOL does not induce a response, and the current fluctuates at a baseline level. This residual fluctuation of the baseline shows the same voltage sensitivity.

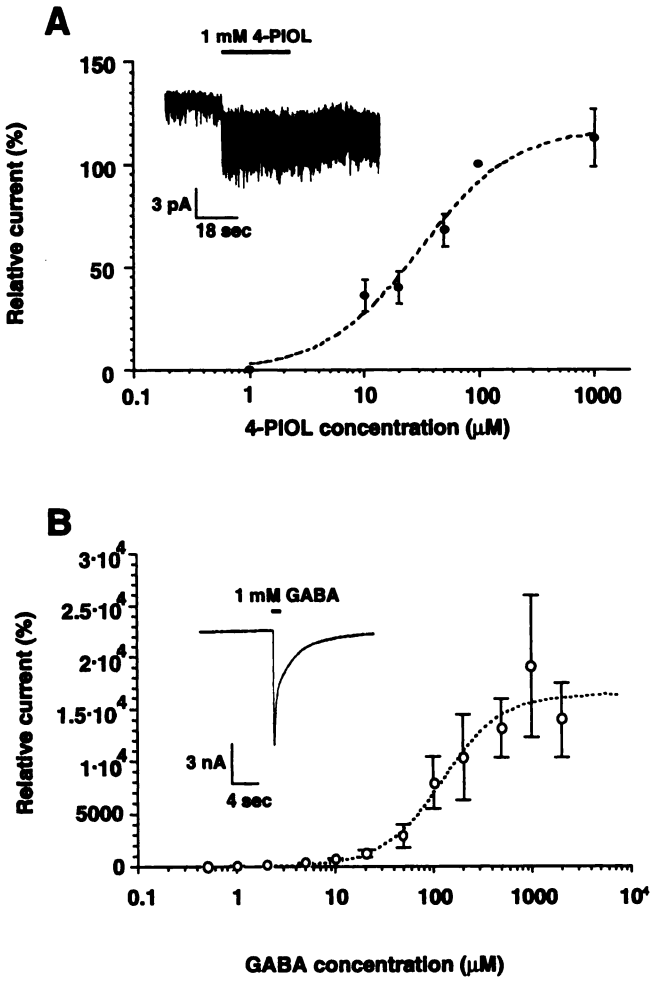

Fig. 3. 4-PIOL is an agonist with low efficacy. A, Concentration-response relationship for 4-PIOL. *Data points*, mean ± standard error for applications of at least 30 sec in 7–13 cells, expressed relative to the response to 100 μM 4-PIOL in the same cell. At this concentration, the mean current value was 6.0 ± 1.0 pA. *Top left*, stretch of a direct current recording showing the characteristic low amplitude response to 1 mM 4-PIOL, which outlasts the duration of the drug application. B, Concentration-response relationship for GABA. Peak current responses to 0.6-sec applications of GABA are expressed relative to the response evoked by 2 μM GABA in the same cell. For each experimental *point*, values are mean ± standard error of responses in 3–10 different cells. The average current at 2 μM is 49 ± 15 pA and corresponds to 0.7% of the maximal response. *Top left*, stretch of direct current recording of the response evoked by 1 mM GABA. Current response fades during the application.

sponses. When 5 μM GABA and 1 mM 4-PIOL were applied simultaneously, the resulting current response was significantly reduced ($p < 0.001$, Student's t test), and the sustained current amplitude was 17 ± 4% of that evoked by 5 μM GABA in the same cell ($n = 7$). The combination of GABA and 4-PIOL elicited a sustained current of 6.9 ± 1.3 pA ($n = 7$ cells), which was not significantly different from the values recorded in 4-PIOL alone (0.1 mM, 0.3 mM, or 1 mM 4-PIOL) in different cells. Thus, 1 mM 4-PIOL eliminated receptor activation induced by 5 μM GABA.

4-PIOL (1 μM) did not affect the current induced by 2 μM GABA ($n = 3$) when the two substances were applied together (not shown), indicating that 4-PIOL concentrations that are ineffective in evoking current responses are also inactive in blocking GABA-evoked responses. Thus, antagonism of GABA-induced responses required detectable agonism at the receptor-channel complex.

In the high micromolar-millimolar range of 4-PIOL concentrations used in the present study, there was little if any evidence of desensitization of the current at either negative or positive potentials during the 1-min-long exposure (Figs. 2 and 3A). Termination of 4-PIOL application was followed by persistence of the low amplitude current response (Fig. 3A), which occurred even when the 4-PIOL pipette was removed from the bath. The latter phenomenon may reflect slow drug dissociation from nonspecific binding sites on the membrane and rebinding to the receptor site.

4-PIOL and GABA Gate Channels with Similar Complex Kinetics, but the Proportions of the Kinetic Components Depend on the Agonist

Spectral density plots derived from fluctuation analysis of Cl^- currents induced by GABA, 4-PIOL, and GABA plus 4-PIOL were consistently fitted by the sum of three Lorentzian components (Figs. 4 and 5 and Table 1), with time constants of 0.5–0.7 msec, 3–6 msec, and 40–70 msec for the first (long-lasting), the second (intermediate-lasting), and the third (short-lasting) components, respectively. There were no statistically significant differences between the two sets of τ values calculated from spectral analysis of the current responses evoked by GABA and 4-PIOL. However, the spectra of 4-PIOL-induced currents revealed a marked prevalence of the shortest-lasting component, whereas spectra of GABA-evoked responses showed that most of the variance was due to the longest-lasting component. The intermediate component made a significantly larger contribution in spectra of noise induced by 5 μM GABA compared with spectra calculated for Cl^- currents evoked by 0.3 mM 4-PIOL. Increasing the 4-PIOL concentration from 0.1 to 1 mM did not induce any significant increase in the σ^2 of each kinetic component, with the total always ~7 pA^2 (Fig. 6). In contrast, increasing the GABA concentration from 0.5 to 5 μM markedly increased the σ^2 of all the three components; on average, the total variance shifted from ~5 to ~50 pA^2. However, the contributions of the longest- and intermediate-lasting components relative to the shortest-lasting component increased with GABA concentration (Fig. 6). The inferred unitary conductance values of GABA- and 4-PIOL-induced channels were not statistically different: 21 ± 1, 21 ± 1, and 21 ± 2 pS, respectively, at 0.5, 1, and 5 μM GABA; 19 ± 4, 19 ± 2, and 17 ± 2 pS, respectively, at 0.1, 0.3, and 1 mM 4-PIOL; and 22 ± 3 pS at 5 μM GABA plus 1 mM 4-PIOL.

4-PIOL-blocked GABA responses exhibited spectra with ratios of exponential components, resembling the spectra of 4-PIOL-evoked responses (Fig. 6 and Table 1). The average absolute value of the variance was markedly lower than the corresponding value evoked by 5 μM GABA and close to those associated with the noise evoked by 4-PIOL. However, some difference was evident relative to the latter and reached statistical significance (Fig. 6). The inferred unitary conductance was not different from the values for GABA and 4-PIOL alone.

We recorded single channels in the outside-out configuration to confirm and extend observations obtained from fluctuation analysis of whole-cell currents (Fig. 7). The preferred main conductance level in the patches was 29 ± 1 pS for both GABA and 4-PIOL. At least one subconductance level of 19 ±

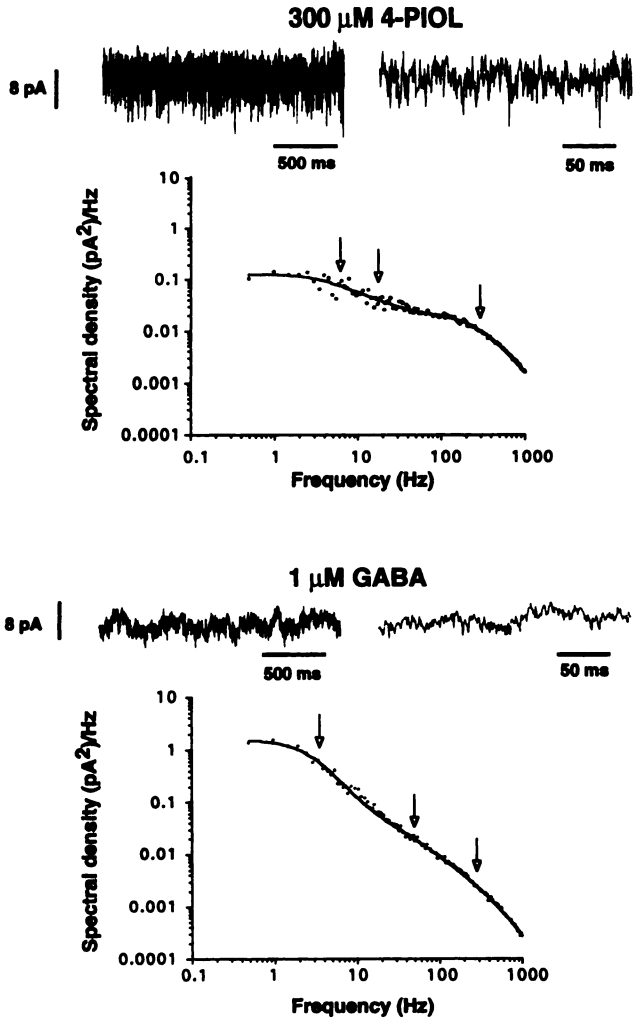

Fig. 4. 4-PIOL and GABA activate Cl^- channels with the same three kinetic components but in different proportions. A, *Top traces*, rapidly fluctuating current response to 300 μM 4-PIOL at different levels of temporal resolution. Spectral analysis of the power distribution over the 0.5–1000 Hz range of frequency reveals that the data points (*dots*) can be fitted by the sum of three Lorentzian equations. *Arrowheads*, corresponding three corner frequencies. There is significant power at the highest frequencies. B, *Top traces*, typical fluctuations in membrane current induced by 1 μM GABA. Spectral analysis reveals corner frequencies similar to those calculated for 4-PIOL spectra but with significantly more power in the lowest frequency component.

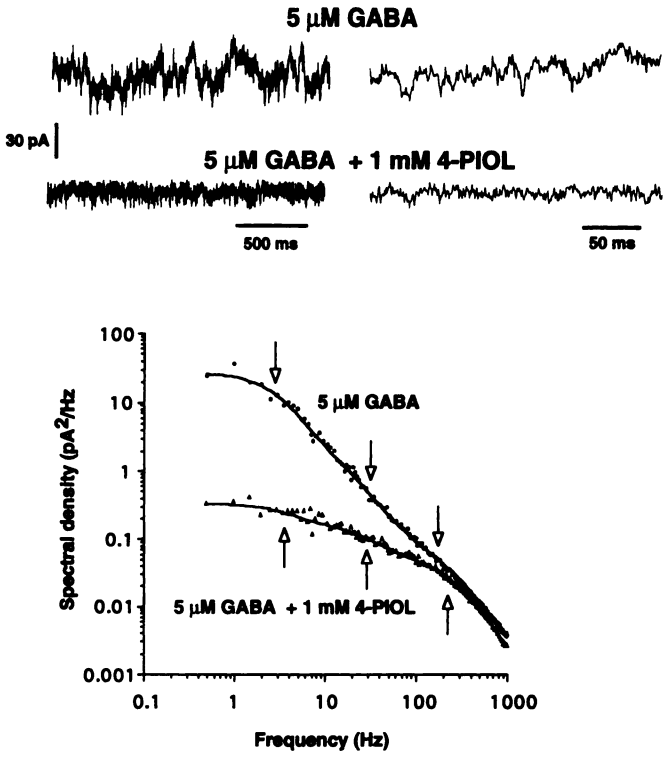

Fig. 5. 4-PIOL blocks GABA-evoked low frequency fluctuations. Membrane current traces show examples of current fluctuations induced in a cell by 5 μM GABA alone and in the presence of 1 mM 4-PIOL. Spectra with baseline noise subtracted are plotted for current responses evoked by GABA and by GABA plus 4-PIOL. Curves are sums of three Lorentzian functions, which have been fitted to the experimental data. *Arrows*, corresponding three corner frequencies. 4-PIOL selectively eliminates power in the two low frequency components.

1 pS occurred periodically for both agonists. The frequency of openings to the 19-pS subconductance state varied in patches from 5% to 30%. Openings to subconductance levels and adjacent closures were excluded from the dwell-time analysis. In one whole-cell recording, where single channels could be resolved at restricted bandwith, we confirmed the main conductance level to be 29 pS for GABA and 4-PIOL.

Results with 1 μM GABA were obtained from four patches with 480, 403, 1597, and 1537 openings. In two of these patches and in a third patch, 300 μM 4-PIOL was tested and gave rise to 1368, 1305, and 2361 openings, respectively. The dwell-time data were calculated both for the individual patches (Fig. 8 and Table 2) and for a pool of events from all patches. The results obtained by the two methods were not significantly different.

The open-time distributions of GABA- and 4-PIOL-activated channels exhibited two components of 0.3–0.4 and 1.4–2 msec. In addition, open-time distribution of GABA had a component of 11 msec, which accounted for 72% of the relative area. The burst-length distribution of GABA-activated channels was fitted by three components with τ values of 0.4, 2.6, and 28 msec, respectively. The longest-lasting component accounted for 82% of the relative area. The burst-length distribution of 4-PIOL-activated channels was fitted by two components with τ values of 0.4 and 2.0 msec, the longest-lasting component representing 66% of the area. The fraction of intraburst time spent in the closed state was 19.4 ± 2.9% and 11.4 ± 5.2% for channels activated by GABA and 4-PIOL, respectively.

Discussion

We have shown in embryonic OB cells that a) 4-PIOL, a structural analog of GABA, blocked GABA-evoked Cl^- currents and induced a low amplitude bicuculline-sensitive Cl^- current; b) 4-PIOL blocked activation by GABA of Cl^- channels only at concentrations that are agonistic; c) the EC_{50} of 4-PIOL for activating the $GABA_A$ receptors on these cells was of the same order of magnitude but lower than that of GABA, whereas the maximal response evoked by GABA was 1000-fold greater than that evoked by 4-PIOL; d) there was no significant difference between the inferred unitary conductances (γ) of GABA- and 4-PIOL-gated channels; e) 4-PIOL and GABA each activated Cl^- channels, the noise spectra of

TABLE 1

The contribution of the three kinetic components depends on agonist structure

	Lorentzian	τ	Contribution
		msec	*%*
0.5 μM GABA (*n* = 8)	First	71 ± 8	51 ± 2[a]
	Second	7.7 ± 1.8	19 ± 1.4[b]
	Third	1.5 ± 0.2	30 ± 2[c]
1 μM GABA (*n* = 6)	First	69 ± 8	53 ± 5[a]
	Second	4.7 ± 0.7	23 ± 4
	Third	0.7 ± 0.1	24 ± 4[c]
5 μM GABA (*n* = 14)	First	66 ± 8	63 ± 5[a]
	Second	7 ± 0.9	22 ± 4
	Third	0.9 ± 0.5	15 ± 2[c]
0.1 mM 4-PIOL (*n* = 6)	First	73 ± 17	3.4 ± 1.2[a]
	Second	6.3 ± 1.1	9.0 ± 3.0[b]
	Third	0.6 ± 0.0	88 ± 3[c,d]
0.3 mM 4-PIOL (*n* = 11)	First	56 ± 11	1.5 ± 0.5[a]
	Second	5.8 ± 1.1	8.8 ± 1.6[b]
	Third	0.6 ± 0.1	90 ± 2[c,d]
1 mM 4-PIOL (*n* = 4)	First	36 ± 6.2	2.5 ± 0.5[a]
	Second	4.8 ± 1.3	10 ± 0.5
	Third	0.6 ± 0.1	88 ± 0.5[c]
GABA plus 4-PIOL (*n* = 7)	First	46 ± 6.4	7.5 ± 1.8[a]
	Second	4.7 ± 0.6	25 ± 2[b]
	Third	0.7 ± 0.0	67 ± 4[c,d]

None of the τ values differed significantly (by analysis of variance) between any concentration or between the two substances. *n* = number of cells analyzed. In the group GABA plus 4-PIOL, 5 μM GABA and 1 mM 4-PIOL were used. Contribution is the relative area of each component. For the contribution of the three components, the only statistically significant differences were the following (analysis of variance, Fisher's PLSD test). First component: [a] Each GABA concentration had a larger contribution than each of the 4-PIOL concentrations and GABA plus 4-PIOL ($p < 0.001$). Second component: [b] 0.5 μM GABA and 0.1 and 0.3 mM 4-PIOL had a lower contribution than GABA plus 4-PIOL ($p < 0.001$). Third component: [c] Each GABA concentration had a lower contribution than each of the 4-PIOL concentrations and the combination of GABA and 4-PIOL ($p < 0.001$). [d] GABA plus 4-PIOL had a lower contribution than 0.1 mM ($p < 0.01$) or 0.3 mM ($p < 0.001$) 4-PIOL.

which had at least three components with time constants that were not significantly different regardless of whether channels were activated by GABA or 4-PIOL; f) 4-PIOL-evoked noise, relative to GABA-evoked noise, exhibited a marked prevalence of the short-lasting component; g) increasing the GABA concentration uniformly increased the variance of each component, whereas even at the highest 4-PIOL concentrations, the variance values of each component remained relatively low; and h) single-channel recordings in outside-out patches demonstrated that the prevalence of fast events inferred in 4-PIOL-induced responses was due to the virtual absence of long-lasting bursts.

Interpretation of Fluctuation Analysis Spectra and Comparison with Kinetic Data Obtained through Single Channel Recordings

Kinetic analysis of single channels in patches is often made difficult by the presence of multiple channels. The condition of no or of a few multiple superimposed events cannot always be fulfilled because $GABA_A$ receptor Cl^- channels can be clustered (8). Therefore, conventional single-channel analysis is limited to patches with few superimposed events, necessitating, for example, only low GABA concentrations or desensitized receptors. The kinetics of very low conductance channels cannot be easily analyzed in single channel recording unless the driving force is markedly increased, the bandwidth is limited, or both. It is difficult to exclude that these manipulations and/or limitations might induce a bias and a

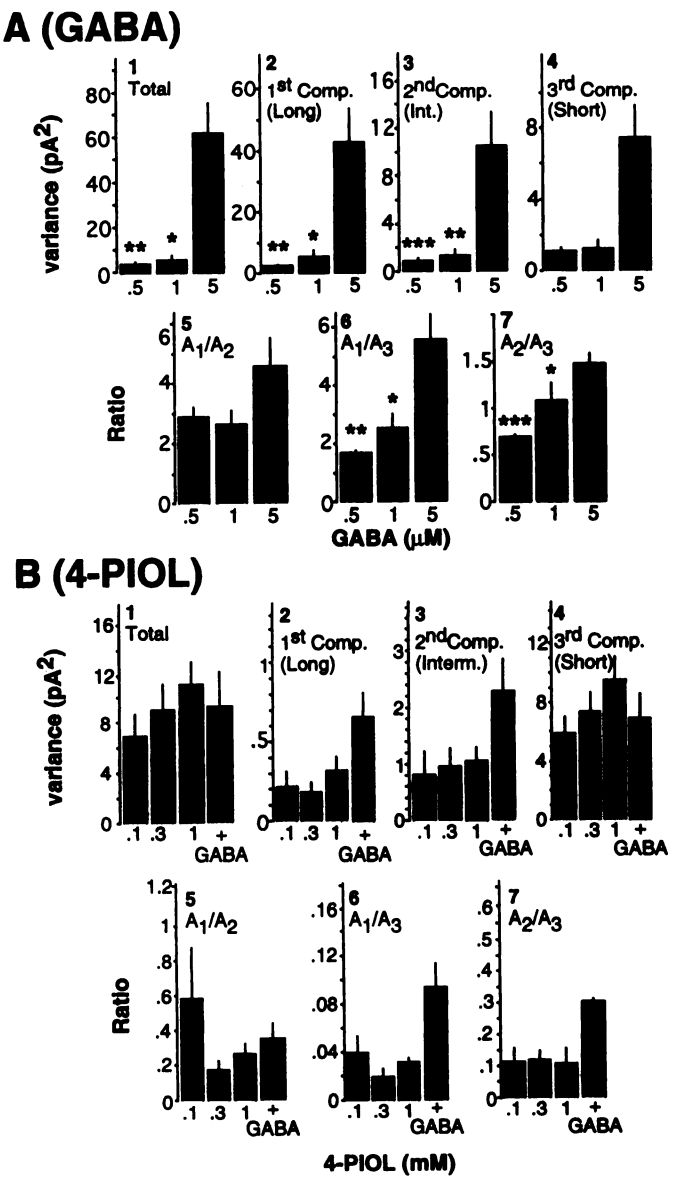

Fig. 6. Different effects of GABA and 4-PIOL concentrations on the kinetics of Cl^- channels inferred from fluctuation analysis. GABA induces a dose-dependent increase in the variance of all three components, whereas at the highest concentrations of the concentration-response relationship the variance of the 4-PIOL-induced noise remains modest. *Columns*, mean values in the variance of the fluctuating signals; *bars*, standard error. Sample size of each group is given on Table 1. A_{1-4} and B_{1-4}, dose-dependent effects of GABA and 4-PIOL on both the total variance and the variance of each component. Increasing the GABA concentration 10-fold (from 0.5 to 5 μM) induces a 10-fold increase in total variance (from 5 to 50 pA^2) and corresponding increases in the variance of each component (differences versus the 5 μM GABA group: *, $p < 0.05$; **, $p < 0.01$; ***, $p < 0.001$, by analysis of variance, Fisher's PLSD test). Increasing the 4-PIOL concentration 10-fold (from 0.1 to 1 mM) does not change variance (~7 pA^2). The addition of 5 μM GABA plus 1 mM 4-PIOL induces a current with a variance (~10 pA^2) that is far lower than the variance of 5 μM GABA-induced noise. A_{5-7}, dose-dependent effects of GABA on the ratios between the areas of the longest-lasting and intermediate-lasting components (A_1/A_2), the areas of the longest-lasting and short-lasting components (A_1/A_3), and the areas of the intermediate-lasting component and the short-lasting components (A_2/A_3) (*, $p < 0.05$, **, $p < 0.01$, ***, $p < 0.001$, by analysis of variance, Fisher's PLSD test). Similar effects of 4-PIOL on the corresponding ratios are not evident when [4-PIOL] is increased 10-fold.

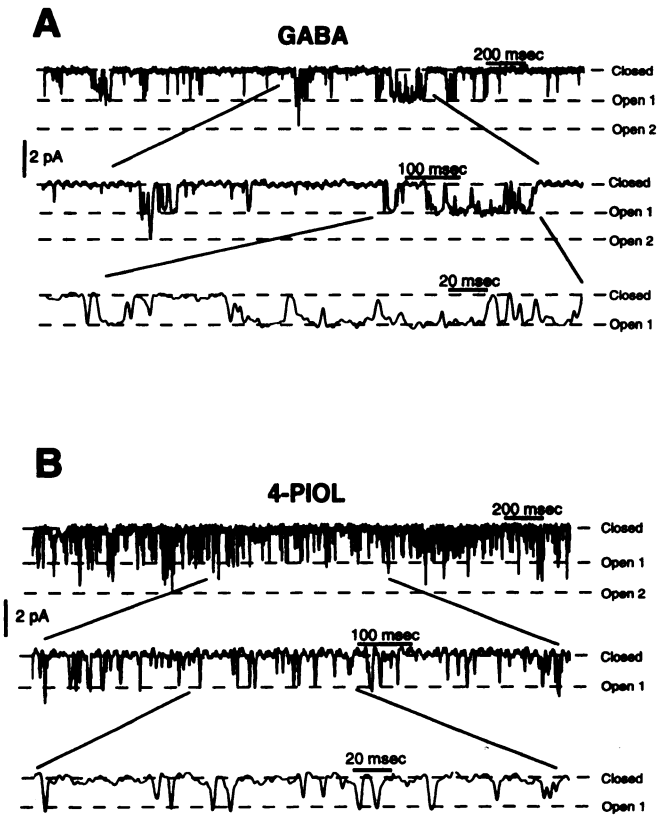

Fig. 7. Single-channel correlates of fluctuating currents. Stretches of single channel currents in excised outside-out patches induced by 1 μM GABA (A) and 0.3 mM 4-PIOL (B) at different time resolutions. GABA-evoked channels open in long duration burst episodes, whereas 4-PIOL induces brief events.

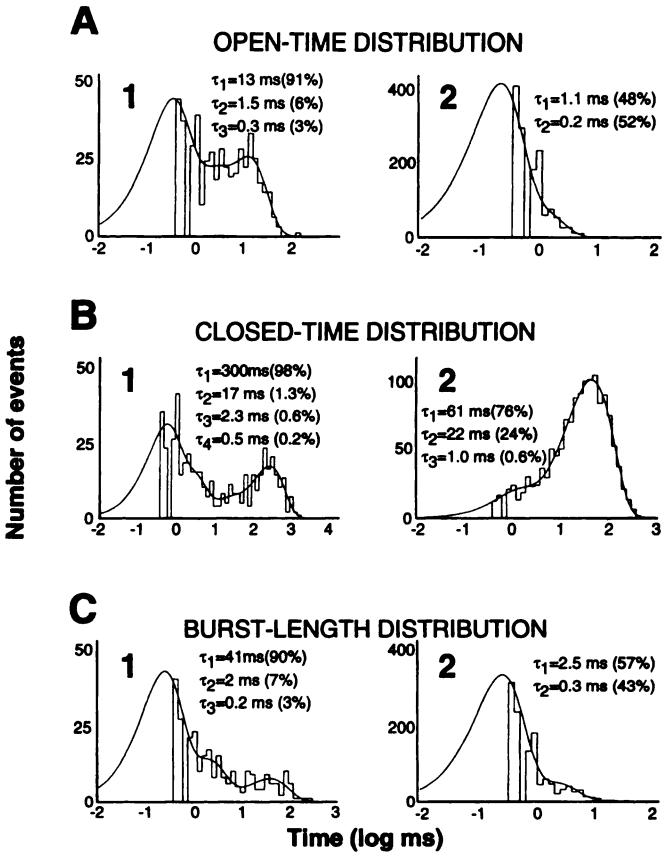

Fig. 8. Open-time distribution, closed-time distribution, and burst-length distributions in the same patches. Data refer to single-channel recordings obtained by the application of 1 μM GABA (A1, B1, and C1) and 300 μM 4-PIOL (A2, B2, and C2), stretches of which have been illustrated in Fig. 7. *Values in parentheses*, relative areas of each τ value. Total recorded times were 66.5 and 70.1 sec for the GABA and 4-PIOL applications, respectively. For GABA, 480 openings, 468 closures, and 278 events in the burst distribution were recorded, whereas for 4-PIOL, 1368 openings, 1363 closures, and 1183 events were recorded. The distributions of the fastest events are distorted by the bandwidth limitations because events shorter than the $<T_r$ are missed; however, the fitting has allowed us to infer the τ of each fast component even when its value is $<T_r$. The intraburst total closed time was 470 msec, corresponding to 10.6% of the total burst duration of the recording.

consequent distortion in measuring and comparing the biophysical properties of channels gated by different ligands. Furthermore, it is useful to compare inferences of the underlying channel properties derived from fluctuation analysis of the macroscopic current recorded whole cell with direct measurement of channel elementary properties in excised patches because patch excision can alter the channel kinetics (9).

Because it is known that GABA-gated Cl^- channels open in bursts (10, 11), the τ of the longest-lasting component estimated by noise analysis is not expected to reflect an open-time distribution but rather to approximate the τ of a burst-length distribution (11–13). This result is confirmed by calculation *a posteriori* of the spectral characteristics that are expected from populations of channels with properties identical to those directly measured in single-channel recordings (see Appendix).

The results obtained from fluctuation analysis of 4-PIOL-evoked noise show that the time constant of the longest-lasting component was not significantly different from the corresponding value derived from spectra of GABA-evoked noise, but the relative contribution was dramatically different. This demonstrates a marked prevalence of slow events in the presence of GABA compared with during exposure to 4-PIOL. Direct measurement of single-channel properties demonstrated that 4-PIOL-evoked channel bursts were mostly composed of one opening with virtually no long-lasting bursts. This indicates *a posteriori* that the spectra of 4-PIOL-evoked noise represent a good approximation of the components of the burst length, that the intermediate- and short-lasting components also correspond to open-time distributions, and that the markedly low contribution of the 4-PIOL long-lasting component is expected to correspond to a markedly low incidence of long-lasting bursts.

Inferences Regarding the Molecular Mechanism of Channel Activation

GABA-gated channels exhibit a dose-dependent multiplication of long-lasting bursts. If the long-lasting component of the spectra is due to bursts with a mean duration close to the time constant of the corresponding Lorentzian function, it is possible to write the equation as follows: $\sigma^2_{GABA}/\sigma^2_{4\text{-PIOL}} = (N_{GABA}\cdot\tau_{GABA}\cdot i^2_{GABA}\cdot ft_{GABA})/(N_{4\text{-PIOL}}\cdot\tau_{4\text{-PIOL}}\cdot i^2_{4\text{-PIOL}}\cdot ft_{4\text{-PIOL}})$ (see Appendix for definitions of N, τ, and Ft); if $ft_{GABA} \approx ft_{4\text{-PIOL}}$ and $i_{GABA} \approx i_{4\text{-PIOL}}$ because $\tau_{GABA} \sim \tau_{4\text{-PIOL}}$ (Table 1), then $\sigma^2_{GABA}/\sigma^2_{4\text{-PIOL}} \sim N_{GABA}/N_{4\text{-PIOL}}$. That is, the ratios of the σ^2 of the long-lasting component of GABA and to 4-PIOL spectra will approximate the

TABLE 2
Summary of single channel results from outside-out patches

Component	1 μM GABA (4 patches)		300 μM 4-PIOL (3 patches)	
	τ	Contribution	τ	Contribution
	msec	%	*msec*	%
Open time 1	0.38 ± 0.03	7.9 ± 1.9	0.30 ± 0.10	32 ± 10
Open time 2	2.0 ± 0.3	20 ± 8	1.43 ± 0.20	68 ± 10
Open time 3	10.7 ± 1.2	72 ± 10		
Closed time 1	0.37 ± 0.05	0.45 ± 0.19	0.79 ± 0.15	0.41 ± 0.15
Closed time 2	3.1 ± 0.8	0.95 ± 0.40	25 ± 8	25 ± 1.3
Closed time 3	19 ± 2	6.9 ± 3.8	82 ± 36	75 ± 1.3
Closed time 4	192 ± 45	92 ± 4		
Burst 1	0.41 ± 0.09	5.8 ± 1.1	0.43 ± 0.16	34 ± 6
Burst 2	2.6 ± 0.3	12 ± 2	2.0 ± 0.3	66 ± 6
Burst 3	28 ± 4	82 ± 3		

Values are mean ± standard error. Contribution is the relative area of each exponential component.

ratio between the numbers of events gated by GABA and 4-PIOL. At the three GABA concentrations used in the present study (0.5, 1, and 5 μM), the σ^2 values of the longest-lasting component (Fig. 6) were ~9-, ~15-, and ~132-fold, respectively, the corresponding values of 4-PIOL-evoked noise. Increasing the GABA concentration also increased the variance of the intermediate- and short-lasting components, which suggests an increase in the frequency of intermediate- and short-lasting bursts; the increase in variance was more pronounced in the long- and intermediate-lasting than in the short-lasting components, indicating a slight but statistically significant higher prevalence of the former kinetic states at higher GABA concentrations. We have inferred that the frequency of long-lasting bursts is higher when GABA rather than 4-PIOL interacts with the $GABA_A$ receptor. Because of their duration, each of the long-lasting bursts contributes more to the total charge transfer than an intermediate- or a short-lasting burst. Therefore, we conclude that the failure of 4-PIOL to induce currents of >7 pA reflects its inability at higher doses to increase the frequency of long-lasting bursts. The complete or nearly complete absence of this kinetic component is bound to have a dramatic effect on the maximal evoked response of an agonist.

4-PIOL low efficacy is not due to the binding of a subset of GABA-gated channels. The possibility that the agonist effect of 4-PIOL might be due to a selective interaction with a specific subset of $GABA_A$ receptors cannot be excluded. However, this seems unlikely because effective antagonism of GABA-induced responses and partial agonism cannot be dissociated and both agonists open channels with virtually identical elementary properties. These results strongly suggest that 4-PIOL and GABA interact with the same $GABA_A$ receptor Cl^- channels. Furthermore, current responses induced by 1 mM 4-PIOL do not desensitize; thus, the low amplitude of the currents induced by 4-PIOL is unlikely to be caused by full agonism on only a very small number of receptor channels.

GABA, 4-PIOL, and the rate of channel openings. At asymptotic 4-PIOL concentrations, in the concentration-response curve the brief and rare channel openings added together generate an average current of ~7 pA. If the proportion of receptor channels occupied by 4-PIOL is comparable with that engaged by GABA, assuming γ = 20 pS, we calculate that the average current evoked by 4-PIOL corresponds to the simultaneous activation of only approximately six channels. This result is consistent with evidence that at the neuromuscular junction, cholinergic agonists with lower efficacy can induce the simultaneous opening of fewer channels than agonists with higher efficacy (reviewed in Ref. 14). Because 4-PIOL blocks GABA-evoked response in a nearly complete manner while inducing only brief and rare events, it must be obstructing the access of GABA to the receptor and therefore is expected to be prevalently bound to the receptor. The closed-time distribution of GABA-evoked channels could be fitted by four components. The two fastest components are within-burst components, and the corresponding τ values are expected to be independent of the number of channels in the patch. The longest-lasting component and the second longest-lasting component might reflect the state of unliganded receptor channel and the state of liganded but shut receptor channel. According to the stochastic theory of a steady state multichannel system (15), in patches containing N channels, if channels are independent from one another and identical to one another, the τ of the longest-lasting component is $1/N$ × the τ value of each individual channel, whereas the τ values of all of the other components are not significantly affected by the number of channels in the patch. If the number of channels in the patch is estimated by the maximum number of multiple superimposed events, the τ values of the longest-lasting component of the closed-time distributions of GABA- and 4-PIOL-gated channels are expected to be 2–3 times the measured values. The time constants of the closed-time distribution have the same order of magnitude, with the τ values of the 4-PIOL distribution lower than the corresponding value of the GABA closed-time distribution. The low intrinsic efficacy of a drug can be explained by a low rate of receptor activation due to the sojourn of the agonist-receptor complex in an inactive state in which the ligand is bound but the receptor is not responding (16). However, the information available in the present study does not allow an easy comparison between the closed time distribution of 4-PIOL- and GABA-evoked channels. In fact, to obtain a number of events practical for distribution analysis, 4-PIOL concentrations close to the EC_{100} were necessary. Because current responses evoked by GABA concentrations of >10 μM were desensitizing, only low concentrations of GABA that elicited ~1% of the maximal response were used as distribution analysis requires steady state conditions. If increasing the ligand concentration increases the frequency of channel openings, this is likely to have resulted in a marked low

incidence of long-lasting closures in the 4-PIOL-gated channels. A component with a τ value of hundreds of msec was evident in the closed-time distribution of the GABA-evoked channels but absent in the closed-time distribution of 4-PIOL-evoked channels. If the weight of the component was sufficiently low to not allow its resolution, this absence could only be apparent.

4-PIOL low efficacy is not due to a channel block mechanism. An alternative explanation for the short-lasting channel openings of 4-PIOL might be a combination of receptor activation with a channel block mechanism, a feature that has been described for agonists at the nicotinic acetylcholine receptor (17). However, although the channel-blocking nicotinic cholinergic agonists are all cations, GABA, 4-PIOL, and many other GABA analogs exist mainly as zwitterions at physiological pH (1). Consequently, they would not be expected to show the same tendency to move into the channel and block the movement of Cl^- ions. Also, a mixed agonist-channel block mechanism is expected to produce concentration-dependent channel kinetics and a reduced current response at high concentrations of agonist-blocker. On the contrary, fluctuation analysis of 0.1–1 mM 4-PIOL-induced macroscopic currents showed no change in τ values or in their relative contributions, and there was no sign of current reduction at high 4-PIOL concentrations. In addition, no current decrease at high 4-PIOL concentrations was observed in cultured hippocampal neurons (18). Furthermore, in the same cell types, 4-PIOL antagonized Cl^- current responses to the full $GABA_A$ agonist isoguvacine in a competitive manner, which is not compatible with a channel block mechanism.

4-PIOL kinetic properties and the biliganded model of the $GABA_A$ receptor. It has been been suggested (19) that short-lasting channel openings and bursts involve the monoliganded state of the $GABA_A$ receptor complex, whereas longer-lasting channel openings and bursts of openings are caused by the biliganded $GABA_A$ receptor. Higher agonist concentrations would increase the probability of the biliganded state; this is in agreement with the experimental observation that in embryonic mammalian spinal neurons cultured for several weeks, the proportion of long-lasting channel openings and bursts increases directly with the agonist concentration (10, 20). Even though the estimated contribution of the intermediate- and short-lasting components of the $GABA_A$ channels studied in the present study is not very accurate (Appendix), the dose-dependent increase in the ratio between the areas of the intermediate- and short-lasting components (A_2/A_3) and in the ratio between the areas of the long- and short-lasting components (A_1/A_3) (Fig. 6A) indicates a dose-dependent interconversion of short events into intermediate- and long-lasting ones, which is consistent with a biliganded model of the $GABA_A$ receptor. High concentrations of 4-PIOL gave rise almost exclusively to short-lasting channel openings, suggesting that the drug preferentially binds the receptor with only one molecule at a time. Consistent with this notion, we found a Hill coefficient close to 1. The absence of any significant difference from the corresponding value for GABA may be due to a desensitization-induced distortion of the GABA concentration-response relationship.

4-PIOL kinetic properties exhibit a distinct mechanism of low efficacy. The Cl^- channel burst-length durations estimated from fluctuation analysis of Cl^- currents induced by GABA and structural analogs range over 10-fold (21). For a series of 12 $GABA_A$ agonists, there is a positive and highly significant correlation between the estimated time constant of the channel burst length and the potency of the agonist in displacing labeled GABA from rat brain membranes in an equilibrium binding assay (22). This suggests that ligands with relatively low potency at $GABA_A$ receptors can activate channels with bursts of relatively short duration. Interestingly, a similar result has been obtained in a study of cholinergic agonists with different efficacies at the neuromuscular junction (reviewed in Ref. 14). Because 4-PIOL gates channels predominantly of very short duration, its kinetic properties show some similarity with this correlation. However, the molecular mechanism related to the differences in agonist potency is different from that suggested in the present study as accounting for the low efficacy of 4-PIOL. The low efficacy of 4-PIOL can be explained as the result of very rare long-lasting open channel transitions and the prevalence of brief ones, with no differences in the mean duration of the burst-length distributions of each component compared with those activated by GABA. The discrepancy might reflect different biophysical mechanisms related to heterogeneity in potency or in efficacy, a mechanism specifically related to the low efficacy of 4-PIOL, or both. The discrepancy might also be due in part to the wider bandwidth of the present patch-clamp study, which has allowed the resolution of several rather than one or two components for these agonists.

Comparison with Binding Studies and the Question of the Desensitized State

Conventional full $GABA_A$ agonists have IC_{50} values for inhibition of ^{3}H-muscimol binding ~1000 times lower than the corresponding EC_{50} values for activation of the receptors. In cultured hippocampal neurons, the EC_{50} for the activation by 4-PIOL of $GABA_A$ receptor Cl^- current was 91 μM (18), whereas the IC_{50} value for inhibition of ^{3}H-GABA binding to rat brain synaptosomes was 6 μM (23). This difference is much smaller than for full agonists. Thus, the difference between binding affinity and effective concentrations could be related to receptor activation and, perhaps, desensitization.

It has been proposed (24) that equilibrium binding experiments at $GABA_A$ receptor are actually measuring the affinity of the ligand to the desensitized receptor. For desensitization to be an energetically favorable process, it must be accompanied by an increase in the affinity of the receptor for the agonist. This can explain the high affinities found for desensitizing full $GABA_A$ agonists in $GABA_A$ receptor binding experiments, whereas the nondesensitizing partial agonist 4-PIOL has a low binding affinity.

Electrophysiological responses to even high concentrations of 4-PIOL do not desensitize, but neither do responses of comparable magnitude to GABA. Because 4-PIOL induces Cl^- current responses preferentially composed of short-lasting channel openings with little if any desensitization, frequent long-lasting channel openings and bursts may be a prerequisite for the desensitization to occur at these receptor channels.

Inferences Regarding Structure-Activity Relationship

The structural requirements for binding to the $GABA_A$ receptor are very strict, and even minor structural alterations in $GABA_A$ agonist molecules often result in a marked or complete loss of affinity (1). Many $GABA_A$ agonists are structurally related analogs of GABA (1). A number of analogs contain a structural element that approximates GABA as part of a cyclic molecule. Embedding the GABA structure in a cyclic domain greatly restricts the conformational flexibility of the molecules. In the relatively potent bicyclic $GABA_A$ agonist THIP, the structure is very rigid, and therefore the conformation of the GABA structural element in THIP is likely to reflect the receptor-active conformation of GABA (1). However, the potency and efficacy of THIP relative to GABA are dependent on the subunit composition of the $GABA_A$ receptor (25), suggesting some variation in receptor-active conformation of GABA among $GABA_A$ receptor subtypes. 4-PIOL contains no GABA structure element, as the number of carbon atoms between the acidic moiety (of the 3-hydroxy-isoxazol ring) and the basic amino group is six, whereas it is only four in GABA. Nevertheless, molecular modeling of the 4-PIOL molecule has shown that it can adopt a folded conformation, in which the acidic and basic moieties can be superimposed on the corresponding moieties of the $GABA_A$ agonist THIP (26). In this L-shaped conformation, the 4-PIOL molecule occupies considerably more space in the agonist-binding domain of the receptor than THIP and GABA. Whether the additional space is responsible for the low frequency of long-lasting bursts and the prevalence of short-lasting openings putatively reflecting monoliganded binding will be tested with new active 4-PIOL analogs.

In conclusion, our biophysical investigation has shown that the low efficacy of 4-PIOL is mostly due to its inability to produce frequent long-lasting bursts and that this may be related to the space occupied by the molecule in the agonist binding domain.

Acknowledgments

We thank Prof. P. Krogsgaard-Larsen and Assoc. Prof. E. Falch, Copenhagen, Denmark, for the gift of 4-PIOL and J. Dempster for providing software for data analysis.

APPENDIX

Even if in a bursting channel fluctuation analysis does not provide an estimate of the channel open time, the technique is still useful for calculating the burst-length distribution. Considering a model proposed for the $GABA_A$ channel kinetics (10) (Fig. 9A), we used data obtained through single-channel recordings to determine the expected properties of the corresponding spectral density plots (13). Single channel recordings indicate the existence of four closed states and three open states. The corresponding noise spectrum is expected to have six rate constants with values equal to the eigenvalues of the relative matrix of transition rates. To simplify calculations, we introduced the following approximations. a) Because channel openings are clustered in three populations of bursts (Table 2), we considered noise spectra to be the sum of three independent processes with an elementary reaction scheme (Fig. 9B); b) Long-lasting bursts are considered to be interrupted by intraburst closures with τ of 3 msec (Table 2); c) Intermediate-lasting bursts are considered to be interrupted by intraburst closures of 0.5 msec (Table 2); d) Because short duration bursts have τ values corresponding approximately to the τ values of fast openings (Table 2), they are considered to be composed by only one opening; e) The mean lifetime of a state is equal to the reciprocal of the sum of transition rates that lead away from that state, but to estimate α and β we assumed that the processes of which α and β are the respective transition rates are considerably faster than all of the other processes leading away from the respective state. We can show that the noise spectra calculated on the basis of these assumptions will lead to a noise-analysis spectra with characteristics similar to those we calculated from experiments in whole-cell recordings. The rate constants of the process are as follows: $\lambda_1 = 0$; $\lambda_2,\lambda_3 = [-b \pm (b^2 - 4ak_2d)^{1/2}]/2$; $b = \beta(K_c + 1) + k_2(c + 1)$; $d = [c/(K_c + 1)/K_c] + 1$. If $1/d = p_3(\infty)$ where $p_3(\infty)$ is the probability of the shut and unliganded receptor at steady state (as in Ref. 13), then at the concentrations used in the present study, $d \sim 1$; $K_c = \alpha/\beta$ (equlibrium constant for conformation change), $c = x_A/K_T$ (normalized concentration), and $K_T = k_2/k_1$ (equilibrium constant for binding to shut channel). $S(f) = 4\gamma(V - V_{eq})m_I[a^{(2)}(-\lambda_2)^{-1}/[1 + (2\pi f/\lambda_2)^2] + a^{(3)}(-\lambda_3)^{-1}/[1 + (2\pi f/\lambda_3)^2]]$; $D = (\lambda_2 + \lambda_3)d/\alpha$; $a^{(2)} = (\lambda_3/\alpha + 1)/D(k_2c/\lambda_3 + 1)$; $a^{(3)} = -(\lambda_2/\alpha + 1)/D(k_2c/\lambda_2 + 1)$.

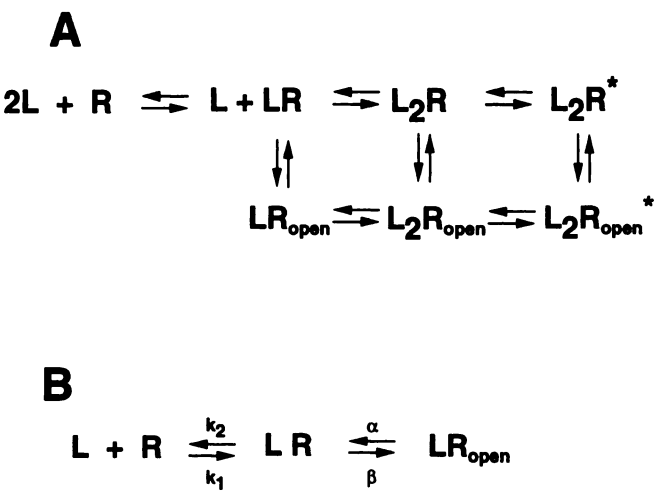

Fig. 9. A, Model assumed to interpret the spectral density plots. B, Simplified versions of the model in A used to calculate the rate constants of spectral density plots.

For GABA in long bursts (Table 2), $1/\alpha = 11$ msec, $\alpha = 91$ sec^{-1}, $1/\beta = 3$ msec, and $\beta = 333$ sec^{-1}. The mean burst length is $(\alpha + \beta)/k_2\alpha = 30$ msec and $k_2 = 158$ sec^{-1} mol^{-1}.

We calculate $\lambda_2 = -26$ sec^{-1}, $\lambda_3 = -556$ sec^{-1}, $\tau_2 = 38$ msec, $a^{(2)} = 0.88$, $\tau_3 = 1.8$ msec, $a^{(3)} = 0.1$, and $a^{(2)}/a^{(3)} \sim 7$. Long-lasting bursts will produce two Lorentzian functions: the time constant of the slow component is close to the mean burst duration and has ~7-fold more power than the fast component. With a similar procedure for intermediate duration burst, we calculate $\lambda_2 = -205$ sec^{-1}, $\lambda_3 = -5075$ sec^{-1}, $\tau_2 = 4.9$ msec, $a^{(2)} = 0.94$, $\tau_3 = 0.2$ msec, $a^{(3)} = 0.06$, and $a^{(2)}/a^{(3)} \sim 16$. Intermediate duration bursts will produce two Lorentzian functions: the time constant of the slow component approximates the mean burst duration and has ~16-fold more power than the fast component. Short-lasting bursts are expected to produce one Lorentzian function with $\tau \sim 0.3$ msec. The spectral density plot is expected to be the sum of five Lorentzian functions. In practice, the fast com-

ponent of intermediate duration bursts will not be observable because of its high frequency and its low weight. To calculate the $S(0)$ of each component, we considered that if each burst of the three populations of bursts was composed of a square pulse corresponding by an uninterrupted opening, the process would produce three Lorentzian functions (long, l; intermediate, i; and short, s) with $\sigma^2_{total} = \sigma_l^2 + \sigma_i^2 + \sigma_s^2$; because $\sigma^2 = m_l \cdot i$, then for the long-lasting Lorentzian function, and similarly for the other Lorentzian functions, $m_l = N_l \cdot \tau_l \cdot i$ and $\sigma_l^2 = N_l \cdot \tau_l \cdot i^2$, where m_l, N_l, τ_l, and σ_l^2 are the macroscopic current, the number of events, the time constant, and the variance corresponding to long-lasting events, respectively. Therefore, $\sigma_l^2:\sigma_i^2:\sigma_s^2 = (N_l \cdot \tau_l):(N_i \cdot \tau_i):(N_s \cdot \tau_s)$. In the burst-length distribution of single-channel recordings, the contribution C_n of each nth component is as follows: $C_n = w_n \cdot \tau_n / (\Sigma w_i \cdot \tau_i) = (N_n \cdot \tau_n)/(\Sigma N_i \cdot \tau_i)$; $C_l:C_i:C_s = (N_l \cdot \tau_l):(N_i \cdot \tau_i):(N_s \cdot \tau_s)$, where w_n and w_i are the amplitudes of the nth and ith components, respectively. Therefore, $\sigma_l^2:\sigma_i^2:\sigma_s^2 = C_l:C_i:C_s$; that is, in the spectra the ratios between the variance values of the different burst-length populations are equal to the ratios between the areas of the components in the single-channel recording of burst-length distribution. We can calculate the ratios of contributions (C) of each component (l, i, and s) of the burst-length distribution relative to the long-lasting component from single-channel recordings, consider the presence of the fast Lorentzian function of long-lasting bursts (long, f), normalize the sum of the four Lorentzian functions to 1 (or 100%), and then solve for the expected contribution of each Lorentzian function in the spectral density plot.

$C_i = 0.15 \cdot C_l$; $C_s = 0.07 \cdot C_l$; $C_l = 7 \cdot C_{long,f}$; $C_l + C_i + C_s + C_{long,f} = 1$, where $C_{long,f}$ is the contribution to the spectrum of the fast Lorentzian function of the longest-lasting bursts. Considering that the variance of each component n is $\sigma_n^2 = (\pi S_0 f_c)/2$, the contribution of each Lorentzian function is $C_n = S(0)_{(n)} \cdot f_{c(n)} / \Sigma(S(0) \cdot f_c)$, and that, on average, at 1 μM GABA $\sigma^2 \approx 5$ pA^2, the value of each $S(0)_{(n)}$ can be determined.

The corresponding spectrum is the sum of four Lorentzian functions, but f_{ci} and $f_{clong,\,f}$ are sufficiently close that recognizing the existence of two distinct processes in the corresponding portion of the spectrum can be difficult. The spectrum calculated for the values indicated above can be fitted with three Lorentzian functions with the following parameters: $f_{cl} = 3.8$ Hz, $C_l = 68\%$; $f_{ci} = 25$ Hz, $C_i = 19\%$; and $f_{cl} = 185$ Hz, $C_s = 13\%$. In fluctuation analysis spectra of GABA-evoked noise, the τ values of the intermediate- and short-lasting components are close to the τ values of bursts obtained in single channel analysis (Table 2), whereas the corresponding relative contributions of A_2 and A_3 are overestimated.

If the kinetics of the 4-PIOL-evoked long-lasting bursting are similar to the kinetics of GABA-evoked long-lasting bursts, the component $C_{long,f}$ of the spectra of 4-PIOL-induced noise is expected to be small enough to be practically negligible. Under these conditions, the contributions of the intermediate- and long-lasting components of the noise spectra are expected to be good approximations of the contribution of the corresponding burst-length distributions. Fluctuation analysis and single-channel analysis results are different in a few additional minor respects: a) the spectra of 4-PIOL-induced currents contained a minor component with a τ of 30–80 msec, which was not observed in the single channel recordings; b) the time constant of the slow component of the burst-length distribution of GABA-evoked Cl^- channels showed a slight but significant difference from the time constant of the low frequency component estimated from spectral analysis of GABA-activated Cl^- current fluctuations; c) the relative contribution of the intermediate- and short-lasting component in the spectra of 4-PIOL-evoked noise was higher than in the corresponding burst-length distribution; and d) the average γ values inferred from fluctuation analysis of whole cell currents were ~30% less than values recorded directly in excised patches with identical concentrations of Cl^- used in both experimental paradigms.

The presence of a minor component with a time constant of 30–70 msec in the spectra of 4-PIOL-induced current variations but not in the single-channel recordings is likely due to the very low contribution of this component to the charge transfer in the total current evoked by 4-PIOL. In the 4-PIOL-induced fluctuations, the spectra indicate that long and brief components contributed by ~3% and ~90%, respectively, to the total variance. Because fluctuation analysis of 4-PIOL-evoked noise is expected to give a good estimate of the channel burst-length distribution, each component of the spectra is due to bursts with a mean duration close to the time constant of the corresponding Lorentzian function. Therefore, it is possible to equate the variance of each component with the product of the elementary current, i, and the mean current, m, produced by each population of bursts ($\sigma^2 = i \cdot m$); if $m = N \cdot \tau \cdot i \cdot ft$, then for each population of bursts $\sigma^2 = N \cdot \tau \cdot i^2 \cdot ft$. That is: $\sigma^2_{short}/\sigma^2_{long} = (N_{short} \cdot \tau_{short} \cdot i^2 \cdot ft_{short})/(N_{long} \cdot \tau_{long} \cdot i^2 \cdot ft_{long}) \approx 90/3$ (see Table 1 and Fig. 6), where N_{short} and N_{long} are the number of short and long bursts, respectively; τ_{short} and τ_{long} are the mean duration of short and long bursts, respectively; i is the channel unitary amplitude; and ft_{short} and ft_{long} are the proportions of intraburst time during which channels are open in short and long bursts, respectively. If in long and short bursts $ft_{short} \approx ft_{long}$ and the channel unitary conductance is similar, in the 4-PIOL-evoked current, the ratio between the number of events of the short- and long-lasting components would be $N_{short}/N_{long} \approx 30 \cdot \tau_{long}/\tau_{short} \approx 3000$. Similarly, it can be calculated $N_{intermediate}/N_{long} \approx 45$, where $N_{intermediate}$ is the number of intermediate duration bursts. Because on average each long burst would be expected to occur only every 3000 short-lasting bursts and every 45 intermediate-lasting bursts, we conclude that in single channel analysis of the kinetics, the existence of a long-lasting component could be easily missed.

The τ value of the longest-lasting component in the single-channel burst-length distribution is slightly lower than the corresponding value of fluctuation analysis, most likely because in single-channel analysis the selection of patches with few multiple superimposed openings is bound to introduce bias into the data. Channels with shorter openings will be less likely to open simultaneously than will channels with long openings. Also, the patch excision from the membrane might have altered some kinetic properties of the channels (9).

In the burst-length distribution of the GABA-activated channels, the relative contributions of the intermediate- and short-lasting components in single-channel recording is lower than those in fluctuation analysis spectra. This is likely due to the presence in the high frequency portion of the spectrum of the fast Lorentzian function of long-lasting

bursts. On the contrary, we cannot give at present a satisfactory explanation for the mismatch of the relative contribution of the intermediate- and short-lasting components between the spectra of 4-PIOL-evoked noise and the corresponding burst-length distribution.

The difference in γ is due in part to the presence of the 19-pS subconductance level. Furthermore, the γ value can be underestimated in fluctuation analysis if a) channels are flickering at frequencies higher than the recording bandwidth, and b) if channels are bursting, the inferred γ is the channel γ multiplied by the fraction of intraburst time in which channels are open (13). The high frequency channel flickering is likely to play a role in the underestimate of the γ of GABA and 4-PIOL-induced channels. However, although bursting channels are open 81% of the time when gated by GABA and 89% of the time when gated by 4-PIOL, the apparent reduction of γ by this mechanism should not exceed 19% and 11%, respectively.

References

1. Krogsgaard-Larsen, P., B. Frolund, F. S. Jorgesen, and A. Schousboe. $GABA_A$ receptor agonists, partial agonists and antagonists: design and therapeutic prospects. *J. Med. Chem.* **37**:2489–2505 (1994).
2. Poulter, M. O., J. L. Barker, A. M. O'Carroll, S. J. Lolait, and L. C. Mahan. Differential and transient expression of $GABA_A$ receptor subunit mRNAs during development of the rat CNS. *J. Neurosci.* **12**:2888–2900 (1992).
3. Poulter, M. O., J. L. Barker, A. M. O'Carroll, S. J. Lolait, and L. C. Mahan. Coexistent expression of $GABA_A$ receptor β_2 β_3 and γ_2 subunit mRNAs during embryogenesis and early postnatal development of the rat CNS. *Neuroscience* **53**:1019–1034 (1993).
4. Paxinos, G., I. Tork, L. H. Tecott, and K. L. Valentino. *Developing Rat Brain*. Academic Press, San Diego (1991).
5. Neher, E., and C. F. Stevens. Conductance fluctuations and ionic pores in membranes. *Ann. Rev. Biophys. Bioeng.* **6**:345–381 (1977).
6. Colquhoun, D., and F. J. Sigworth. Fitting and statistical analysis of single channel records, in *Single-Channel Recording* (B. Sakmann and E. Neher, eds.). Plenum Press, New York, 191–263 (1983).
7. Colquhoun, D., and B. Sakmann. Fast events in single-channel currents activated by acetylcholine and its analogs at the frog muscle end-plate. *J. Physiol. (Lond.)* **369**:501–557 (1985).
8. Caruncho, H. J., G., Puia, E., Slobodyansky, P. Pinto da Silva, and E. Costa. Freeze-fracture immunocytochemical study of the expression of native and recombinant $GABA_A$receptors. *Brain Res.* **603**:234–242 (1993).
9. Covarrubias M., and J. H. Steinbach. Excision of membrane patches reduces the mean open time of nicotinic acetylcholine receptors. *Pflugers Arch.* **416**:385–392 (1990).
10. Macdonald, R. L., C. J. Rogers, and R. E. Twyman. Kinetic properties of the $GABA_A$ receptor main conductance state of the mouse spinal cord neurons in culture. *J. Physiol. (Lond.)* **410**:479–499 (1989).
11. Newland, C. F., and S. Cull-Candy. On the mechanism of action of picrotoxin on GABA receptor channels in dissociated sympathetic neurons of the rat. *J. Physiol. (Lond)* **447**:191–213 (1992).
12. Neher, E., and J. H. Steinbach. Local anaesthetics transiently block currents through single acetylcholine-receptor channels. *J. Physiol. (Lond.)* **277**:153–176 (1978).
13. Colquhoun, D., and A. G. Hawkes. Relaxation and fluctuations of membrane currents that flow through drug-operated ion channels. *Proc. R. Soc. Lond. B Biol. Sci.* **199**:231–262 (1977).
14. Colquhoun, D. The link between drug binding and response: theories and observations, in *The Receptors: A Comprehensive Treatise* (R. D. O'Brien, ed.). Plenum Press, New York, 93–142 (1979).
15. Kijima, S., and H., Kijima. Statistical analysis of channel current from a membrane patch. II: a stochastic theory of a multi-channel system in the steady-state. *J. Theor. Biol.* **128**:435–455 (1987).
16. Pallotta, B. S. Single ion channel's view of classical receptor theory. *FASEB J.* **5**:2035–2043 (1991).
17. Ogden, D. C., and D. Colquhoun. Ion channel block by acetylcholine, carbachol and suberyldicholine at the frog neuromuscular junction. *Proc. R. Soc. Lond. B Biol. Sci.* **225**:329–355 (1985).
18. Kristiansen, U., J. D. C. Lambert, E. Falch, and P. Krosgaard-Larsen. Electrophysiological studies of the $GABA_A$ receptor ligand 4-PIOL on cultured hippocampal neurons. *Br. J. Pharmacol.* **104**:85–90 (1991).
19. Jackson, M. B., H. Lecar, D. A. Mathers, and J. L. Barker. Single channel currents activated by GABA, muscimol and (−)pentobarbital in cultured mouse spinal neurons. *J. Neurosci.* **2**:889–894 (1982).
20. Mathers, D. A., and Y. Wang. Effect of agonist concentration on the lifetime of GABA-activated membrane channels in spinal cord neurons. *Synapse* **2**:627–632 (1988).
21. Barker, J. L., and D. A. Mathers. GABA analogs activate channels of different duration in cultured mouse spinal neurons. *Science* **212**:358–361 (1981).
22. Barker, J. L., N. L. Harrison, and D. G. Owen. Pharmacology and physiology of Cl^- conductances activated by GABA in cultured mammalian central neurons, in *Chloride Channels and Carriers in Nerve, Muscle, and Glial Cells*. (F. J. Alvarez-Leefmans and J. M. Russell, eds.). Plenum Publishing Corp., New York, 273–297 (1990).
23. Krogsgaard-Larsen, P., B. Frolund, U. Kristiansen, J. D. C. Lambert, E. Falch, and D. R. Curtis. Novel $GABA_A$ agonists and partial agonists, in *Transmitter Amino Acid Receptors: Structures, Transduction and Models for Drug Development* (E. A. Barnard and E. Costa, eds.). FIDIA Research Symposium Series, Thieme Medical Publishers, New York, 449–458 (1992).
24. Lohse, M. J. Molecular mechanisms of membrane receptor desensitization. *Biochim. Biophys. Acta* **1179**:171–188 (1993).
25. Ebert, B., K. A. Wafford, P. J. Whiting, P. Krogsgaard-Larsen, and J. A. Kemp. Molecular pharmacology of $GABA_A$ receptor agonists and partial agonists in oocytes injected with different α, β and γ receptor subunit combinations. *Mol. Pharmacol.* **46**:957–963 (1994).
26. Byberg Buur, J. R., H. Hjeds, P. Krogsgaard-Larsen, and F. S. Jorgensen. Conformational analysis and molecular modelling of a partial $GABA_A$ agonist and a glycine antagonist related to the $GABA_A$ agonist THIP. *Drug Design Discovery* **10**:213–229 (1993).

Send reprint requests to: Dr. Ruggero Serafini, Laboratory of Neurophysiology, National Institute of Neurological Disorders and Stroke, National Institutes of Health, Bldg. 36, Room 2C-02, Bethesda, MD 20892.